Inorganica Chimica Acta 363 (2010) 4080–4087

Contents lists available at ScienceDirect

Inorganica Chimica Acta

journal homepage: www.elsevier.com/locate/ica

Nickel(II) and copper(II) complexes of Schiff base ligands containing N_4O_2 and N_4S_2 donors with pyrrole terminal binding groups: Synthesis, characterization, X-ray structures, DFT and electrochemical studies

Ali Akbar Khandar [a,*], Christine Cardin [b], Seyed Abolfazl Hosseini-Yazdi [a], John McGrady [c], Marjan Abedi [a], Seyed Amir Zarei [a], Yu Gan [b]

[a] Department of Inorganic Chemistry, Faculty of Chemistry, University of Tabriz, Tabriz 51666-14766, Iran
[b] Department of Chemistry, University of Reading, Whiteknights, Reading RG6 6AD, UK
[c] Department of Chemistry, University of Oxford, OX1 3QR, UK

ARTICLE INFO

Article history:
Received 7 July 2010
Received in revised form 4 August 2010
Accepted 11 August 2010
Available online 19 August 2010

Keywords:
Copper(II) complexes
Nickel(II) complexes
X-ray structure
Pyrrol-2-carboxaldehyde
Cyclic voltammetry
DFT calculations

ABSTRACT

A series of hexadentate ligands, H_2L^m ($m = 1–4$), [1*H*-pyrrol-2-ylmethylene]{2-[2-(2-{[1*H*-pyrrol-2-ylmethylene]amino}phenoxy)ethoxy]phenyl}amine (H_2L^1), [1*H*-pyrrol-2-ylmethylene]{2-[4-(2-{[1*H*-pyrrol-2-ylmethylene]amino}phenoxy)butoxy]phenyl} amine (H_2L^2), [1*H*-pyrrol-2-ylmethylene][2-({2-[(2-{[1*H*-pyrrol-2-ylmethylene]amino}phenyl)thio]ethyl}thio)phenyl]amine (H_2L^3) and [1*H*-pyrrol-2-ylmethylene][2-({4-[(2-{[1*H*-pyrrol-2-lmethylene]amino}phenyl)thio]butyl}thio) phenyl]amine (H_2L^4) were prepared by condensation reaction of pyrrol-2-carboxaldehyde with {2-[2-(2-aminophenoxy)ethoxy]phenyl}amine, {2-[4-(2-aminophenoxy)butoxy] phenyl}amine, [2-({2-[(2-aminophenyl)thio]ethyl} thio)phenyl]amine and [2-({4-[(2-aminophenyl)thio]butyl}thio)phenyl]amine respectively. Reaction of these ligands with nickel(II) and copper(II) acetate gave complexes of the form ML^m ($m = 1–4$), and the synthesized ligands and their complexes have been characterized by a variety of physico-chemical techniques. The solid and solution states investigations show that the complexes are neutral. The molecular structures of NiL^3 and CuL^2, which have been determined by single crystal X-ray diffraction, indicate that the NiL^3 complex has a distorted octahedral coordination environment around the metal while the CuL^2 complex has a seesaw coordination geometry. DFT calculations were used to analyse the electronic structure and simulation of the electronic absorption spectrum of the CuL^2 complex using TDDFT gives results that are consistent with the measured spectroscopic behavior of the complex. Cyclic voltammetry indicates that all copper complexes are electrochemically inactive but the nickel complexes with softer thioethers are more easily oxidized than their oxygen analogs.

1. Introduction

Schiff base ligands and their complexes have been studied extensively with the aim of shedding light on various aspects of catalytic activity [1–5], magnetic, spectroscopic and anticancer properties [6–11] as well as the role of metal ions in biological systems [12–14]. The active sites of many metalloenzymes contain nickel and copper, and the transition metals play important roles in controlling the catalytic function [15–18]. The relationship between the structure and the chelate ring size of multidentate ligands in coordination compounds is a subject of considerable importance because the coordination chemistry of the metals is affected by the both the type of donor atom and steric requirements [19]. Although salicylidimine ligands and their complexes have been extensively studied in this context, relatively little is known about the Schiff base ligands, especially those derived from pyrrole-2-carboxaldehyde that can potentially act as hexadentate donors [20–33]. Previously, we have considered the strain effects in the copper and nickel complexes of two such Schiff base ligands (Scheme 1), each of which possesses an N_2O_4 donor set [34]. In the case where two methylene groups separate the ether oxygen atoms the coordination geometry is distorted square planar geometry but the more flexible analog with four methylene groups between the ether oxygen atoms acts as a hexadentate donor giving a distorted octahedral geometry. Herein, we report the synthesis and characterization of copper(II) and nickel(II) complexes of the new ligands H_2L^1, H_2L^2, H_2L^3 and H_2L^4 (Scheme 2) which are structurally related to those in Scheme 1 [34] but with different donor sets of atoms, N_4O_2 and N_4S_2, and with pyrrole terminal moieties derived from pyrrole-2-carboxaldehyde and {2-[2-(2-aminophenoxy)ethoxy]phenyl}amine (**1**), {2-[4-(2-aminophenoxy)

* Corresponding author. Tel.: +98 (411) 3346494; fax: +98 (411) 3340191.
E-mail addresses: khandar@tabrizu.ac.ir, akhandar@yahoo.com (A.A. Khandar).

0020-1693/$ - see front matter © 2010 Elsevier B.V. All rights reserved.
doi:10.1016/j.ica.2010.08.019

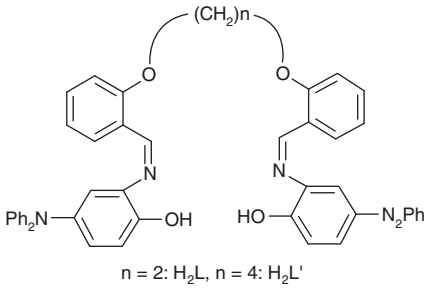

Scheme 1. Structure representation of Schiff base ligands H_2L and H_2L'.

butoxy] phenyl}amine (**2**), [2-({2-[(2-aminophenyl)thio]ethyl} thio)phenyl]amine (**3**) and [2-({4-[(2-aminophenyl)thio]butyl} thio)phenyl]amine (**4**), respectively. We report the crystal structures of NiL^3 and CuL^2 and discuss the effects of different donor atom type, chelate size and the nature of the terminal binding groups on the coordination chemistry of the ligands.

2. Experimental

2.1. Materials

The solvents and reagents used in these studies were obtained from commercial sources and were used as received.

2.2. Physical measurements

Elemental analyses were carried out using an Elemental Vario EL III instrument. ^1H NMR and ^{13}C NMR spectra were recorded at 400.13 and 100 MHz on a Bruker Avance 400 spectrometer in $CDCl_3$ using Me_4Si as the internal reference. Cyclic voltammetric measurements were performed using an Auto lab potentiostat PGSTAT 302 ECO CHEMIE. In all electrochemical studies a three-electrode system was used, consisting of a glassy carbon working electrode, a platinum wire auxiliary electrode, and Ag/AgCl as the reference electrode. All of the electrochemical experiments were carried out under an argon atmosphere at room temperature using dimethyl formamide solution of complexes containing 0.1 M lithium perchlorate as the supporting electrolyte. IR spectra were recorded on a Bruker Tensor 27 FT-IR spectrometer as KBr pellets. Electron impact (70 eV) mass spectrum was recorded on a Shimadzu, QP1100EX spectrometer. Electronic spectra were recorded on a Shimadzu, UV-1650 PC spectrophotometer from solution in dichloromethane. Conductivity data were measured in DMF on a Metrohem 712 conductometer instrument.

2.3. X-ray crystallography

Relevant data about the collections and structure solutions are summarized in Table 1. Crystals of NiL^3 and CuL^2 for X-ray crystallography were grown by slow evaporation of acetonitrile/chloroform and ethanol/dichloromethane (1:1) solution, respectively. The data sets were collected on a Bruker SMART CCD detector for NiL^3 and on an Oxford Diffraction Gemini-S-Ultra diffractometer for CuL^2 using φ and ω scans. For the NiL^3 complex a fine-focus sealed tube was used as the radiation source. Data reduction for NiL^3 was carried out using the program SAINT [35]. An absorption correction for NiL^3 was applied using SADABS [36]. The CuL^2 complex crystallized as needle-shaped crystals that were very thin and therefore weakly diffracting. The data were therefore collected at low temperature (150 K) at station 9.8, Daresbury SRS (UK) using synchrotron radiation source at a wavelength of 0.68829 Å. The structures were determined by direct methods and were refined by full-matrix least-squares procedures using the SHELXTL [37]. Scattering factors were taken from International Tables for crystallography [38].

2.4. Syntheses

2.4.1. Diamines (*1*–*4*)

{2-[2-(2-Aminophenoxy)ethoxy]phenyl}amine (**1**) and {2-[4-(2-aminophenoxy)butoxy] phenyl}amine (**2**) were synthesized according to the published procedure [39].

[2-({2-[(2-Aminophenyl)thio]ethyl}thio)phenyl]amine (**3**) and [2-({4-[(2-aminophenyl)thio]butyl}thio)phenyl]amine (**4**) were prepared by a modification of a literature method [40]. In each case 2-aminothiophenol (60 mmol) was dissolved in ethanol (15 cm^3), then 6 cm^3 of NaOH aqueous solution (40%) was added. The yellow-brown mixture was stirred and heated at reflux for 20 min. 1,2-Dibromoethane (5.64 g, 30 mmol) and 1,4-dibromobutane (6.48 g, 30 mmol) were added dropwise to the solution. The solution was refluxed for 2 h. In the case of (**3**) the resulting solution was cooled in water and the precipitate was filtered and recrystallized from water/ethanol to give the white product. Yield: 2.49 g, 30%. M.p. 77–78 °C. Selected FT-IR data (cm^{-1}, KBr): 3290s and 3355s (NH), 3056w (CH_{arom}), 2925w (CH_{aliph}), 1617s and 1476s ($C{=}C_{arom}$). In the case of (**4**) the resulting solution was extracted with water/chloroform. This product is liquid in room temperature. Yield: 2.74 g, 70%. Selected FT-IR data (cm^{-1}, KBr): 3453s and 3353s (NH), 3016w and 3056w (CH_{arom}), 2923w (CH_{aliph}), 1611s and 1478s ($C{=}C_{arom}$).

2.4.2. Ligands

2.4.2.1. [(1Z)-1H-Pyrrol-2-ylmethylene]{2-[2-(2-{[(1Z)-1H-pyrrol-2-ylmethylene]amino} phenoxy)ethoxy]phenyl}amine (H_2L^1). A solution of pyrrole-2-carboxaldehyde (0.9510 g, 10 mmol) in ethanol

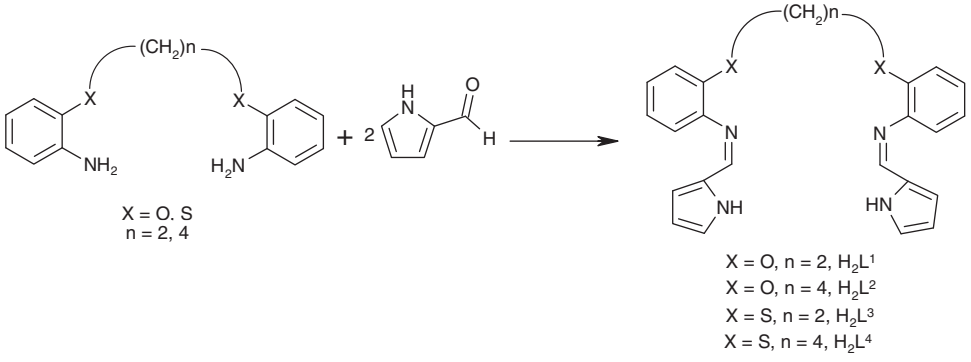

Scheme 2. Synthesis and structure representation of Schiff base ligands H_2L^1, H_2L^2, H_2L^3 and H_2L^4.

Table 1
Crystallographic data for NiL^3 and CuL^2.

	NiL^3	CuL^2
Formula	$C_{24}H_{20}N_4NiS_2$	$C_{104}H_{96}Cu_4{\cdot}N_{16}O_8$
Formula weight	487.27	1952.13
T (K)	293(2)	150(2)
Crystal color	orange	brown
Crystal size (mm)	0.55 × 0.45 × 0.25	0.1 × 0.02 × 0.02
Crystal system	trigonal	monoclinic
Space group	$P3(2)21$	$P2(1)/c$
a (Å)	8.9429(3)	25.037(3)
b (Å)	8.9429(3)	13.8374(18)
c (Å)	23.2577(19)	28.095(4)
α (°)	90	90
β (°)	90	108.062(2)
γ (°)	120	90
V (Å^3)	1610.85(15)	9254(2)
Z	3	4
D_{calc} (Mg/m^3)	1.507	1.401
λ (Å)	0.71073	0.68829
μ (mm^{-1})	1.118	0.975
Reflections collected/ unique	18 631/3141 (R_{int} = 0.0280)	109 336/30 107 (R_{int} = 0.0715)
F(0 0 0)	756	4048
θ range for data collection (°)	2.63–30.01	1.52–31.52
Index ranges	$-12 \leqslant h \leqslant 12$, $-12 \leqslant k \leqslant 12$, $-31 \leqslant l \leqslant 32$	$-35 \leqslant h \leqslant 35$, $-20 \leqslant k \leqslant 20$, $-40 \leqslant l \leqslant 40$
Data/restraints/ parameters	3141/0/142	30 107/0/1304
Goodness-of-fit (GOF) on F^2	1.008	1.002
Final R indices ($I > 2\sigma(I)$)	R_1 = 0.0299, wR_2 = 0.0773	R_1 = 0.0470, wR_2 = 0.0980
R indices (all data)	R_1 = 0.0368, wR_2 = 0.0827	R_1 = 0.0962, wR_2 = 0.1146
Largest difference in peak and hole (e Å^{-3})	0.846 and −0.161	0.607 and −0.783

$R_1 = [\Sigma||F_o| - |F_c||]/\Sigma|F_o|$ (based on F), $wR_2 = \{[\Sigma w\,(|F_o^2 - F_c^2|)^2]/[\Sigma w(F_o^2)^2]\}^{1/2}$ (based on F^2).

(10 cm^3) was added dropwise to a solution of (**1**) (1.2214 g, 5 mmol) in warm ethanol (30 cm^3) in the dark. The solution was refluxed for 24 h. Then the solution was cooled and evaporated at room temperature, the product precipitated as a cream solid which was recrystallized from ethanol. Yield: 1.0011 g, 50.25%. M.p. 74–75 °C. Selected FT-IR data (cm^{-1}, KBr): 3266m ($NH_{pyrrole}$), 2930w (CH_{aliph}), 1617s (C=N), 1583s and 1495s (C=C_{arom}). *Anal.* Calc. for $C_{24}H_{22}N_4O_2$: C, 72.34; H, 5.57; N, 14.06. Found: C, 72.48; H, 5.40; N, 14.20%. ^{1}H NMR data (400.13 MHz, $CDCl_3$, Me_4Si): δ 4.39 (4H, s, alkyl), 6.23–7.17 (14H, m, arom), 8.25 (2H, s, imine). ^{13}C NMR data (100 MHz, $CDCl_3$, Me_4Si): δ 65.68, 65.74, 108.97, 110.92, 111.006, 116.86, 117.96, 120.64, 123.32, 125.34, 129.85, 151.12, 151.12. UV–Vis [λ_{max}/nm (ε/M^{-1} cm^{-1})]: 333 (36 120), 302 (28 280), 242 (23 820) in CH_2Cl_2.

2.4.2.2. [(1Z)-1H-Pyrrol-2-ylmethylene]{2-[4-(2-{[(1Z)-1H-pyrrol-2-ylmethylene] amino}phenoxy)butoxy]phenyl}amine (H_2L^2). This ligand was prepared by a similar method to H_2L^1 using pyrrole-2-carboxaldehyde (0.9510 g, 10 mmol) and (**2**) (1.3617 g, 5 mmol), but the solution was refluxed for 12 h. The resulting yellow oil was triturated with diethyl ether to give a cream solid which was collected by filtration. Yield: 0.4905 g, 23%. M.p. 148–149 °C. Selected FT-IR data (cm^{-1}, KBr): 3222m ($NH_{pyrrole}$), 3077w (CH_{arom}), 2936w (CH_{aliph}), 1623s (C=N), 1584s and 1493s (C=C_{arom}). *Anal.* Calc. for $C_{26}H_{26}N_4O_2$: C, 73.22; H, 6.14; N, 13.14. Found: C, 73.10; H, 6.31; N, 12.98%. ^{1}H NMR data (400.13 MHz, $CDCl_3$, Me_4Si): δ 1.94 (4H, s, alkyl), 4.03 (4H, s, alkyl), 6.13–7.15 (14H, m, arom), 8.24 (2H, s, imine), 11.63 (2H, s, br, H-pyrrole). ^{13}C NMR data (100 MHz, $CDCl_3$, Me_4Si): δ 25.13 (C, s, alkyl), 68.25 (C, s, alkyl), 108.65, 113.29, 115.80, 118.74, 120.42, 123.24, 125.17, 129.58, 141.33, 150.01, 151.51 (s, 22C, arom, imine). UV–Vis [λ_{max}/nm (ε/M^{-1} cm^{-1})]: 334 (28 900), 299 (31 900), 227 (20 240) in CH_2Cl_2.

2.4.2.3. [(1Z)-1H-pyrrol-2-ylmethylene][2-({2-[(2-{[(1Z)-1H-pyrrol-2-ylmethylene] amino}phenyl)thio]ethyl}thio)phenyl]amine (H_2L^3). A solution of pyrrole-2-carboxaldehyde (0.9510 g, 10 mmol) in ethanol (10 cm^3) was added dropwise to a solution of (**3**) (1.3821 g, 5 mmol) in warm ethanol (15 cm^3) in the dark. The solution was stirred and heated under reflux for 24 h. The solution was evaporated at room temperature. The resulting yellow oil was dissolved in the minimum amount of CH_2Cl_2 and was precipitated by adding of *n*-hexane. The product was collected by filtration and recrystallized from CH_2Cl_2 to *n*-hexane. Yield: 0.6459 g, 30%. M.p. 96–97 °C. Selected FT-IR data (cm^{-1}, KBr): 3208m ($NH_{pyrrole}$), 2975w (CH_{alyph}), 1621s (C=N), 1569s (C=C_{arom}). *Anal.* Calc. for $C_{24}H_{22}N_4S_2$: C, 66.94; H, 5.15; N, 13.01. Found: C, 67.12; H, 5.14; N, 12.91%. ^{1}H NMR data (400.13 MHz, $CDCl_3$, Me_4Si): δ 3.1 (4H, s, alkyl), 6.27–7.32 (14H, m, arom), 8.15 (2H, s, imine), 10.22 (2H, s, br, H-pyrrole). UV–Vis [λ_{max}/nm (ε/M^{-1} cm^{-1})]: 310 (44 820), 280 (36 300), 257 (27 460), 232 (27 740) in CH_2Cl_2. Mass spectral parent ion: m/z 431.

2.4.2.4. [(1Z)-1H-pyrrol-2-ylmethylene][2-({4-[(2-{[(1Z)-1H-pyrrol-2-ylmethylene] amino}phenyl)thio]butyl}thio)phenyl]amine (H_2L^4). This ligand was prepared by a similar method to that of H_2L^3 using pyrrole-2-carboxaldehyde (0.9510 g, 10 mmol) and (**4**) (1.5224 g, 5 mmol). In this case, a brown oil was obtained that was triturated with diethylether to give the product as a brown solid which was separated by filtration. Yield: 0.9861 g, 43%. M.p. 157–158 °C. Selected FT-IR data (cm^{-1}, KBr): 3272m ($NH_{pyrrole}$), 3010w (CH_{arom}), 2928w (CH_{aliph}), 1615s (C=N), 1566s (C=C_{arom}). *Anal.* Calc. for $C_{26}H_{26}N_4S_2$: C, 68.09; H, 5.71; N, 12.22. Found: C, 68.23; H, 5.68; N, 12.29%. ^{1}H NMR data (400.13 MHz, $CDCl_3$, Me_4Si): δ 1.8–1.84 (4H, q, alkyl), 2.91–2.94 (4H, t, alkyl), 6.24–7.30 (14H, m, arom), 8.16 (2H, s, imine), 10.10 (2H, s, br, H-pyrrole). UV–Vis [λ_{max}/nm (ε/M^{-1} cm^{-1})]: 305 (48 800), 277 (44 020), 254 (32 640), 236 (30 300) in CH_2Cl_2.

2.4.3. Copper(II) and nickel(II) complexes

All nickel(II) and copper(II) complexes of the ligands were prepared by addition of a solution of nickel acetate tetrahydrate (0.1245 g, 0.5 mmol) or copper acetate monohydrate (0.0998 g, 0.5 mmol) in ethanol (25 cm^3) to a solution of H_2L^1 and H_2L^2 and to a suspension of H_2L^3 and H_2L^4 (0.5 mmol) in absolute ethanol (25 cm^3). In each case the precipitate was filtered and recrystallized from CH_3CH_2OH/CH_2Cl_2 for NiL^1, NiL^2, NiL^3, CuL^1, CuL^2 and CuL^3 and from THF/$(C_2H_5)_2O$ for NiL^4 and CuL^4.

2.4.3.1. NiL^1. Reaction time: 4 h. Color: brown. Yield: 0.1707 g, 75%. M.p. > 290 °C (dec). Selected FT-IR data (cm^{-1}, KBr): 3068w (CH_{arom}), 2937w (CH_{aliph}), 1558s (C=N). *Anal.* Calc. for $C_{24}H_{20}NiN_4O_2$: C, 63.34; H, 4.43; N, 12.31. Found: C, 63.38; H, 4.30; N, 12.25%. UV–Vis [λ_{max}/nm (ε/M^{-1} cm^{-1})]: 410 (46 020), 278 (28 160), 264 (28 980), 227 (20 460), 1004 (18) in CH_2Cl_2. Λ_m = 1.6 Ω^{-1} cm^2 mol^{-1} in DMF.

2.4.3.2. NiL^2. Reaction time: 4 h. Color: red-brown. Yield: 0.2150 g, 89%. M.p. > 300 °C (dec). Selected FT-IR data (cm^{-1}, KBr): 3067w (CH_{arom}), 2932w (CH_{aliph}), 1557s (C=N). *Anal.* Calc. for $C_{26}H_{24}NiN_4O_2$: C, 64.63; H, 5.01; N, 11.60. Found: C, 64.71; H, 4.90; N, 11.67%. UV–Vis [λ_{max}/nm (ε/M^{-1} cm^{-1})]: 406 (42 840), 331 (12 900), 256 (16 140), 231 (19 000), 1030 (22) in CH_2Cl_2. Λ_m = 1.8 Ω^{-1} cm^2 mol^{-1} in DMF.

2.4.3.3. NiL³. Reaction time: 4 h. Color: red. Yield: 0.2046 g, 84%. M.p. > 310 °C (dec). Selected FT-IR data (cm^{-1}, KBr): 3064w (CH_{arom}), 2925w (CH_{aliph}), 1540s (C=N). *Anal.* Calc. for $C_{24}H_{20}NiN_4S_2$: C, 59.16; H, 4.14; N, 11.50. Found: C, 59.22; H, 4.03; N, 11.42%. UV–Vis [λ_{max}/nm (ε/M^{-1} cm^{-1})]: 439 (51 220), 424 (52 940), 339 (9800), 270 (8500), 231 (27 720), 849 (23) in CH_2Cl_2. Λ_m = 1.5 Ω^{-1} cm^2 mol^{-1} in DMF.

2.4.3.4. NiL⁴. Reaction time: 4 h. Color: green. Yield: 0.2293 g, 89%. M.p. > 310 °C (dec). Selected FT-IR data (cm^{-1}, KBr): 3057w (CH_{arom}), 2925w (CH_{aliph}), 1549s (C=N). *Anal.* Calc. for $C_{26}H_{24}NiN_4S_2$: C, 60.60; H, 4.69; N, 10.87. Found: C, 60.48; H, 4.82; N, 10.78%. UV–Vis [λ_{max}/nm (ε/M^{-1} cm^{-1})]: 440 (24 080), 417 (31 040), 271 (8420), 230 (19 500), 873 (23) in CH_2Cl_2. Λ_m = 2.7 Ω^{-1} cm^2 mol^{-1} in DMF.

2.4.3.5. CuL¹. Reaction time: 2 h. Color: brown. Yield: 0.2070 g, 90%. M.p. > 260 °C (dec). Selected FT-IR data (cm^{-1}, KBr): 3098w (CH_{arom}), 2927w (CH_{aliph}), 1568s (C=N). *Anal.* Calc. for $C_{24}H_{20}CuN_4O_2$: C, 62.67; H, 4.38; N, 12.18. Found: C, 62.54; H, 4.49; N, 12.15%. UV–Vis [λ_{max}/nm (ε/M^{-1} cm^{-1})]: 381 (38 300), 309 (15 260), 244 (22 380), 232 (22 220), 624 (146) in CH_2Cl_2. Λ_m = 3.1 Ω^{-1} cm^2 mol^{-1} in DMF.

2.4.3.6. CuL². Reaction time: 2 h. Color: brown. Yield: 0.2123 g, 87%. M.p. > 270 °C (dec). Selected FT-IR data (cm^{-1}, KBr): 3057w (CH_{arom}), 2929w (CH_{aliph}), 1558s (C=N). *Anal.* Calc. for $C_{26}H_{24}CuN_4O_2$: C, 63.99; H, 4.96; N, 11.48. Found: C, 64.05; H, 4.87; N, 11.44%. UV–Vis [λ_{max}/nm (ε/M^{-1} cm^{-1})]: 378 (41 500), 307 (17 700), 244 (24 540), 232 (25 900), 602 (131) in CH_2Cl_2. Λ_m = 2.2 Ω^{-1} cm^2 mol^{-1} in DMF.

2.4.3.7. CuL³. Reaction time: 2 h. Color: dark green. Yield: 0.1968 g, 80%. M.p. > 160 °C (dec). Selected FT-IR data (cm^{-1}, KBr): 3066w (CH_{arom}), 2923w (CH_{aliph}), 1568s (C=N). *Anal.* Calc. for $C_{24}H_{20}CuN_4S_2$: C, 58.58; H, 4.10; N, 11.38. Found: C, 58.65; H, 3.97; N, 11.29%. UV–Vis [λ_{max}/nm (ε/M^{-1} cm^{-1})]: 400 (27 900), 253 (19 840), 232 (23 820), 635 (157) in CH_2Cl_2. Λ_m = 8.8 Ω^{-1} cm^2 mol^{-1} in DMF.

2.4.3.8. CuL⁴. Reaction time: 2 h. Color: green. Yield: 0.2263 g, 87%. M.p. > 150 °C (dec). Selected FT-IR data (cm^{-1}, KBr): 3057w (CH_{arom}), 2922w (CH_{aliph}), 1559s (C=N). *Anal.* Calc. for $C_{26}H_{24}CuN_4S_2$: C, 60.04; H, 4.65; N, 10.77. Found: C, 60.12; H, 4.53; N, 10.80%. UV–Vis [λ_{max}/nm (ε/M^{-1} cm^{-1})]: 381 (28 760), 291 (18 200), 251 (22 200), 231 (24 260), 618 (209) in CH_2Cl_2. Λ_m = 2.3 Ω^{-1} cm^2 mol^{-1} in DMF.

2.5. Computational method

The gas phase geometry of the CuL^2 complex was optimized in the doublet state using density functional theory (B3LYP functional) as implemented in GAUSSIAN 98 [41–43]. The calculations were performed using the 6-311G(d) basis set for the metal center, 6-31G(d) for the donor atoms, and 3-21G for all remaining atoms [44]. No symmetry constraints were applied in the calculations. The electronic spectrum of the CuL^2 complex was calculated using TDDFT starting from the optimized ground-state geometry in the gas phase using the same B3LYP functional and basis sets [45].

3. Results and discussion

3.1. Synthesis and characterization

The hexadentate Schiff base ligands H_2L^1, H_2L^2, H_2L^3 and H_2L^4 have been synthesized according to Scheme 2 and characterized by IR, elemental analysis, ^1H NMR, ^{13}C NMR, UV–Vis spectra and mass spectroscopy only for the H_2L^3. The IR and NMR data are in accordance with the proposed structures. Disappearance of the C=O and NH_2 stretching vibrations, related to aldehyde and diamine functional groups, respectively along with the growth of a strong band in the region of 1615–1623 cm^{-1} due to the C=N bonds, indicate the formation of the Schiff base ligands. The peaks in the region 8.15–8.25 ppm in the ^1H NMR spectra of the ligands are assigned to the resonance of the azomethine protons (CH=N), also confirming the formation of the Schiff base ligands.

The reaction of the ligands with copper(II) and nickel(II) acetate in a 1:1 ratio in ethanol gives CuL^m and NiL^m complexes. The elemental analyses are consistent with the proposed molecular formula that show the ratio of metal/ligand is 1:1. All complexes in ca. 10^{-3} M solutions in DMF at 25 °C have very low conductance, indicating that the complexes are all neutral [46]. Thus the ligands must act as doubly negatively charged anions in complexation to Cu(II) and Ni(II) ions. This hypothesis is supported by the absence of pyrrole N–H stretches in the FT-IR spectra of the complexes. Therefore, two nitrogen atoms of pyrrole groups are deprotonated prior to complexation. The metals are also bound to ligands through the azomethine nitrogens, deduced from the observed decrease in C=N stretching frequency, 49–65 cm^{-1} and 59–81 cm^{-1} upon complexation of ligands to Cu(II) and Ni(II) ions respectively. On going from CuL^m complexes to the NiL^m analogs the C=N stretching frequency decreases by 10, 1, 28 and 10 cm^{-1}, respectively. In Cu(II) complexes the C=N stretching frequencies for CuL^1 and CuL^3 and for CuL^2 and CuL^4 are the same. On the other hand the C=N frequency difference between CuL^1 and CuL^2 is the same as that between CuL^3 and CuL^4. So it seems that the difference in each pair depends only on the length of the aliphatic linkage and the nature of the donor atom (S or O) has relatively little impact. In the Ni (II) complexes, NiL^1 with NiL^3 and NiL^2 with NiL^4, in contrast, the C=N stretching frequencies are very different, suggesting that in this case the O or S atoms of the ligands are in the coordination sphere of the Ni (II) ion. This assumption is supported by single crystal X-ray structures of CuL^2 and NiL^3 complexes (*vide infra*) which show six coordination for Ni but four coordination for Cu. These results are also consistent with the electronic spectra of the complexes. UV–Vis spectra of the ligands and their complexes were studied in dichloromethane, at 5×10^{-5} M concentration in the 190–500 nm window and 10^{-2} M in the 400–1100 nm window. All the ligands, H_2L^m, have similar spectral features in the short wavelength region: the maxima of the bands corresponding to the $\pi \rightarrow \pi^*$ and $n \rightarrow \pi^*$ transition are observed at 333, 334, 310 and 305 nm and 302, 299, 280 and 277 nm for H_2L^m (m = 1–4), respectively. These bands show a distinct red shift in complexation. The electronic spectra for CuL^m (m = 1–4) complexes also show a broad shoulder in the visible region (620–670 nm), assigned to the d–d transition ($d_{xz,yz} \rightarrow d_{x^2-y^2}$ and $d_z^2 \rightarrow d_{x^2-y^2}$) of Cu(II) ion based on TDFT and DFT calculations. This spectral feature is typical of the square planar coordination geometry [47,48] revealed by X-ray crystallography for CuL^2. The nickel complexes, NiL^m, exhibit a broad absorption band centered in 1004, 1030, 849 and 873 nm for m = 1–4, respectively. These bands can be assigned to $^3A_{2g} \rightarrow {}^3T_{2g}$ transition in an octahedral ligand field [22,32], which is constructed from two nitrogen atoms of the pyrrole groups, two nitrogens of azomethines and two etheric oxygens or two thioetheric sulfurs. These transitions correspond to

Δ_O = 9960, 9708, 11 779 and 11 455 cm^{-1}, respectively, indicating ligands with N_4O_2 donor set have weaker ligand fields than their analogs with an N_4S_2 set. The results also indicate that the ligand field strength decreases when the aliphatic linkage in the ligands is elongated. In our earlier paper [34] we assumed that the ligand H_2L in Scheme 1 would be unable to form six coordinated complexes with an N_2O_4 donor set due to the short length of the dimethylene bridge. However, the new results with Ni(II) suggest that this is not the case. Moreover, ligands similar to those of Schemes 1 and 2 with phenol and naphthol terminal groups with dimethylene linkage act as a hexadentate ligand type $O_2N_2O_2$ or $O_2N_2S_2$ toward the Ni(II) ion [49], in good agreement with our results. Therefore, it is obvious that the length of the aliphatic linkage in these ligands is not always a defining factor in complexation geometry, and the nature of the metal ion and terminal groups are also important.

3.2. Structural studies

The crystal structure of the NiL^3 complex with atomic numbering is illustrated in Fig. 1(A). Selected bond distances and bond angles are listed in Table 2. The molecular structure of the complex has a distorted octahedral geometry around the Ni(II) center, as can be judged from the spread in its observed angles [81.54(6)–99.41(6)°] and the trans angles [178.60(9)–164.41(4)°]. The Ni(II) ion is bound through the N_4S_2 atoms, where both the imine nitrogens are disposed *trans* to each other with a bond angle of 178.60(9)° and both thioether sulfur atoms and also both two pyrrole nitrogens occupy the cis coordination sites with bond angles of 87.36(2)° and 96.09(9)°, respectively. The Ni–N (imine) (2.0315(13) Å) and Ni–N (pyrrole) (2.0308(16) Å) bond lengths are comparable to corresponding

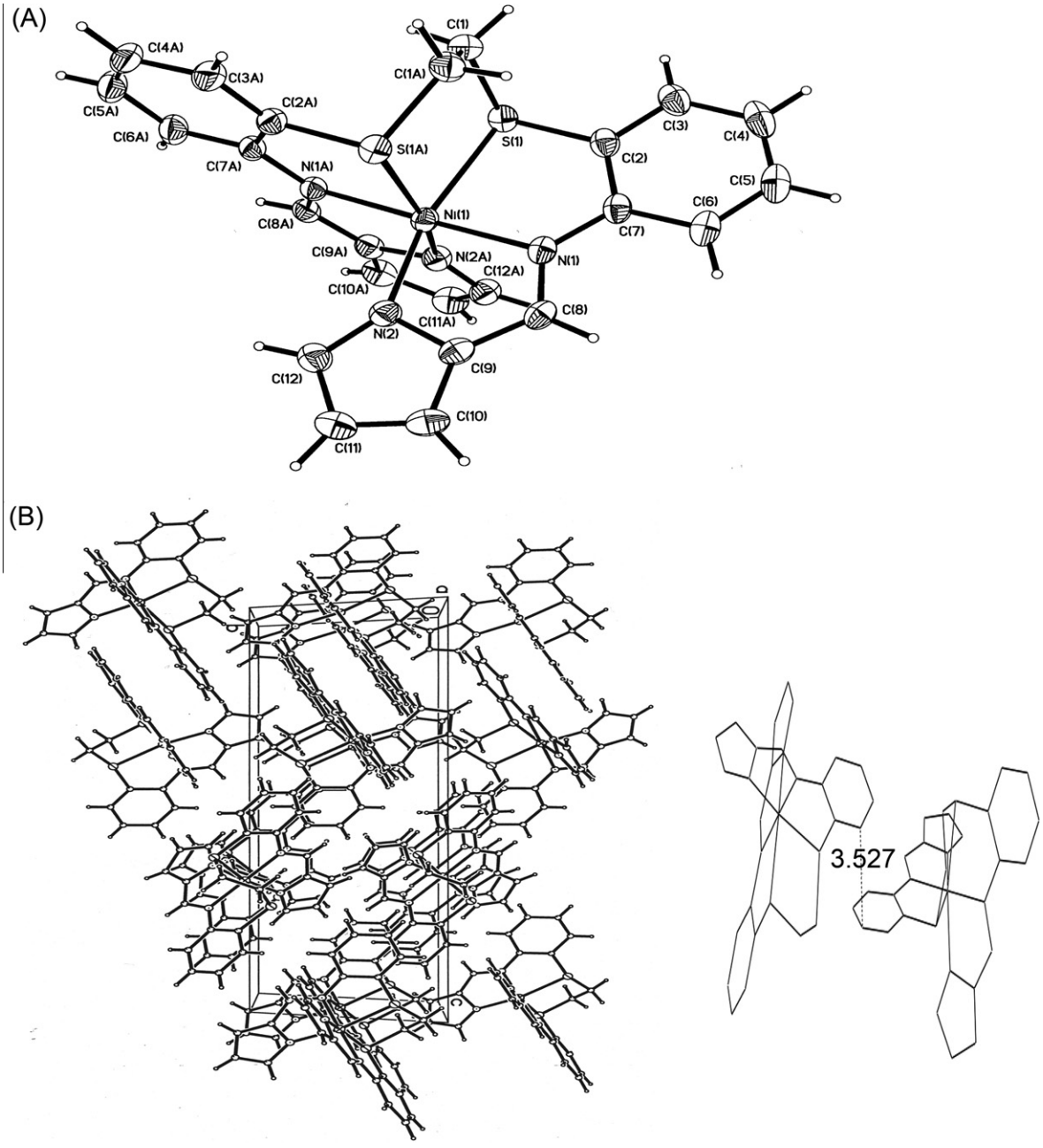

Fig. 1. ORTEP drawing with atom labeling (A) and packing structure diagram (B) for NiL^3.

Table 2
Selected bond lengths (Å) and bond angles (°) for NiL^3.

Bond lengths			
Ni(1)–N(1)	2.0315(13)	N(1)–C(8)	1.308(2)
Ni(1)–N(1A)	2.0315(13)	N(2)–C(9)	1.376(2)
Ni(1)–N(2)	2.0308(16)	N(2)–C(12)	1.337(2)
Ni(1)–N(2A)	2.0308(16)	S(1)–C(1)	1.818(2)
Ni(1)–S(1)	2.4336(5)	S(1)–C(2)	1.7856(18)
Ni(1)–S(1A)	2.4336(5)	C(2)–C(7)	1.411(3)
N(1)–C(7)	1.399(2)	C(8)–C(9)	1.403(3)
C(1)–C(1A)	1.504(5)		
Bond angles			
N(1)–Ni(1)–N(1A)	178.60(9)	N(1A)–Ni(1)–S(1A)	83.37(5)
N(1)–Ni(1)–S(1A)	95.61(4)	N(1A)–Ni(1)–S(1)	95.61(4)
N(1)–Ni(1)–S(1)	83.37(5)	N(2A)–Ni(1)–N(2)	96.09(9)
N(2)–Ni(1)–N(1)	81.54(6)	N(2A)–Ni(1)–N(1)	99.41(6)
N(2)–Ni(1)–N(1A)	99.41(6)	N(2A)–Ni(1)–N(1A)	81.54(6)
N(2)–Ni(1)–S(1A)	90.22(4)	N(2A)–Ni(1)–S(1A)	164.41(4)
N(2)–Ni(1)–S(1)	164.41(4)	N(2A)–Ni(1)–S(1)	90.22(4)
S(1A)–Ni(1)–S(1)	87.36(2)		

distances reported in the literature [34,50] and the Ni–S (2.4336(5) Å) bond length is comparable to the mean value of the corresponding distances in Ref. [30]. The metric parameters of the NiL^3 complex molecule show that a twofold axis bisects the complex, passing through the C1–C(1A) bond and the Ni atom. $Z = 3$ in the $P3(2)21$ space group reveals that the molecular symmetry axis is also the symmetry axis of the crystal. Complexation of the H_2L^3 ligand with Ni results in the formation of five-membered chelate rings. The crystal packing of NiL^3 illustrated in Fig. 1(B) shows ligand–ligand interactions between C11···H(1A) and C4···C8 of adjacent molecules with distances of 2.874 and 3.382 Å, respectively. The aromatic rings stack with adjacent ones in an offset face-to-face fashion with an interplanar angle of 18.56° and shortest atom–atom distance of 3.57 Å. The mean centroid–centroid distance of 4.271 Å indicates weak interactions between phenyl rings.

The structure of CuL^2 is given in Fig. 2. Relevant bond distances and angles are given in Table 3. There are four different molecules

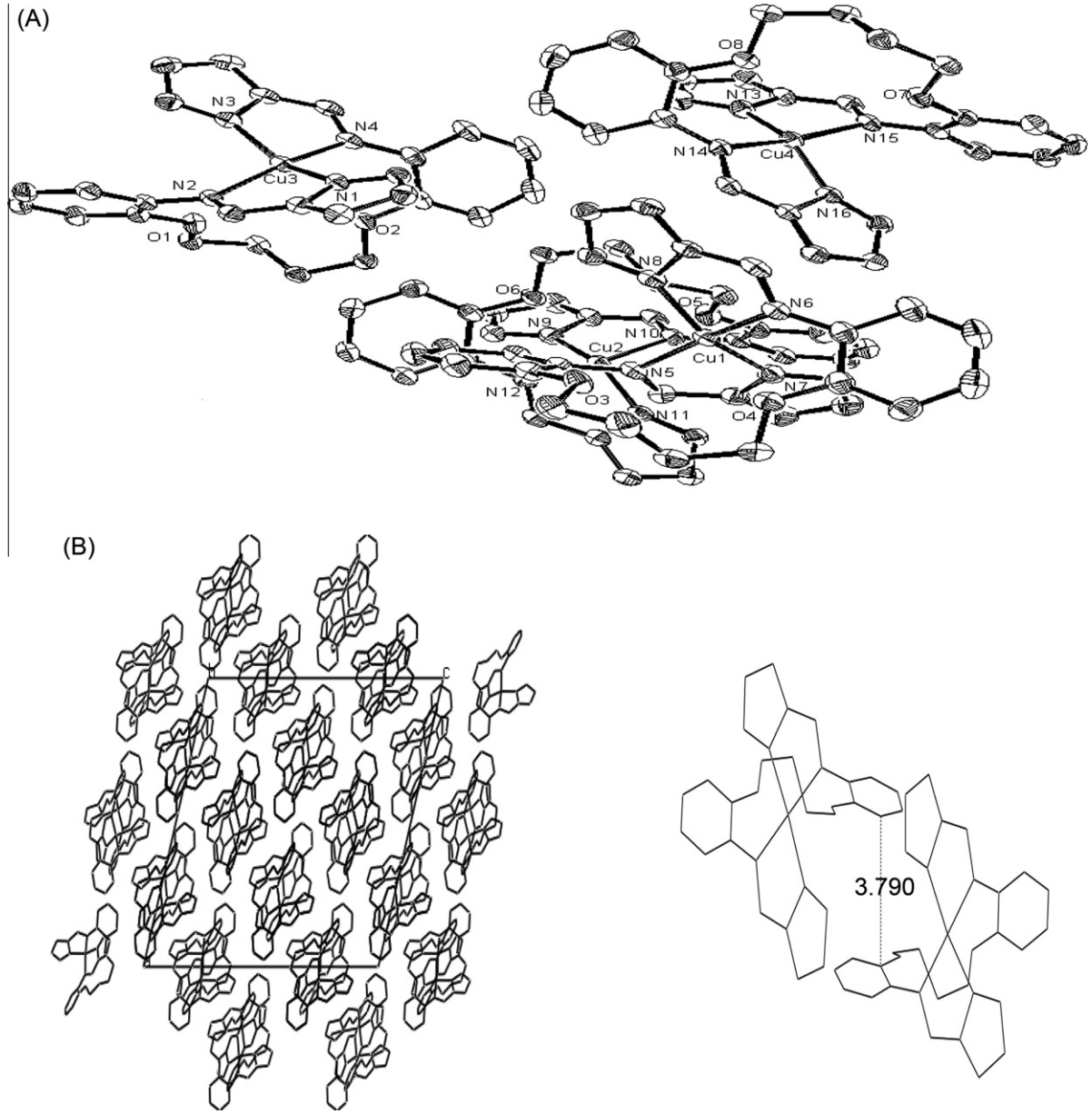

Fig. 2. ORTEP drawing (A) (hydrogen atoms are omitted for clarity) and packing structure diagram along the *c* crystallographic axis (B) for CuL^2 complex.

Table 3
Selected bond lengths (Å) and bond angles (°) for CuL^2.

Bond lengths			
Cu(1)–N(5)	1.9909(18)	Cu(3)–N(1)	1.9560(19)
Cu(1)–N(6)	2.0207(19)	Cu(3)–N(2)	1.9979(18)
Cu(1)–N(7)	1.9559(19)	Cu(3)–N(3)	1.9548(19)
Cu(1)–N(8)	1.9677(19)	Cu(3)–N(4)	2.0020(18)
Cu(2)–N(9)	1.9437(19)	Cu(4)–N(13)	1.9516(19)
Cu(2)–N(10)	2.0063(18)	Cu(4)–N(14)	1.9980(18)
Cu(2)–N(11)	1.9421(19)	Cu(4)–N(15)	1.9883(18)
Cu(2)–N(12)	1.9998(17)	Cu(4)–N(16)	1.9468(19)
Bond angles			
N(7)–Cu(1)–N(8)	152.12(8)	N(3)–Cu(3)–N(1)	148.43(8)
N(7)–Cu(1)–N(5)	82.72(8)	N(3)–Cu(3)–N(2)	100.04(8)
N(8)–Cu(1)–N(5)	99.19(8)	N(1)–Cu(3)–N(2)	83.24(7)
N(7)–Cu(1)–N(6)	100.59(8)	N(3)–Cu(3)–N(4)	82.52(8)
N(8)–Cu(1)–N(6)	82.40(8)	N(1)–Cu(3)–N(4)	100.58(8)
N(5)–Cu(1)–N(6)	169.88(8)	N(2)–Cu(3)–N(4)	168.37(7)
N(11)–Cu(2)–N(9)	151.66(8)	N(16)–Cu(4)–N(13)	152.24(8)
N(11)–Cu(2)–N(12)	82.80(8)	N(16)–Cu(4)–N(15)	98.69(8)
N(9)–Cu(2)–N(12)	99.02(8)	N(13)–Cu(4)–N(15)	82.98(8)
N(11)–Cu(2)–N(10)	100.61(8)	N(16)–Cu(4)–N(14)	83.03(8)
N(9)–Cu(2)–N(10)	82.89(8)	N(13)–Cu(4)–N(14)	101.60(8)
N(12)–Cu(2)–N(10)	169.19(8)	N(15)–Cu(4)–N(14)	166.90(8)

Table 4
The selected structural parameters of CuL^2 calculated by DFT and their X-ray observed values for comparison (distances in (Å), angles in (°)).

Parameter	X-ray	DFT
$Cu–N_{pyrrole}$	1.9421–1.9677	1.97
$Cu–N_{imine}$	1.9880–2.0207	2.022
$N_{imine}–Cu–N_{imine}$	166.90(8)–169.88(8)	167.07
$N_{pyrrole}–Cu–N_{imine}$	82.40(8)–82.98(7)	83.27
	99.19(8)–100.04(8)	100.56
	100.59(8)–101.60(8)	100.58
	82.72(8)–83.24(7)	83.28
$N_{pyrrole}–Cu–N_{pyrrole}$	148.43(8)–152.24(8)	145.76

in this structure that show no element of symmetry in the solid state. Coordination around the copper(II) ions is defined by the N_4 donor set of the H_2L^2 ligand. In each copper the two imine and the two pyrrole nitrogen atoms of the potentially hexadentate ligand are arranged in a distorted square planar environment with bond distances of 1.9421–1.9677 Å for $Cu–N_{py}$ and 1.9880–2.0207 Å for $Cu–N_{imine}$. The weak interactions between etheric oxygens and copper ion are reflected in Cu···O distances of approximately 3 Å, and the angles between adjacent bonds in the coordination sphere of copper are in the range 82.40–101.60°. The copper(II) ions and two imine nitrogens lie out of the mean planes defined by N(7)N(8)Cu(1)N(5)N(6), N(9)N(11)Cu(2)N(10)N(12), N(1)N(3)Cu(3)N(2)N(4) and N(13)N(16)Cu(4)N(14)N(15) by distances of (0.118, 0.291, 0.298), (0.115, 0.300, 0.306), (0.132, 0.334, 0.335) and (0.096, 0.317, 0.328) Å, respectively, while the two pyrrole nitrogens are displaced to the opposite side of these mean planes by distances of (0.353, 0.355), (0.359, 362), (0.398, 0.403) and (0.366, 0.375) Å, respectively. The coordination geometry can be views as a tetrahedral distortion of the square planar geometry, or better as a seesaw structure, with the nearly linear N (imine)–Cu–N (imine) angle forming the plank and the N (pyrrole)–Cu–N (pyrrole) angle the pivot. The values of the structural index τ_4 (defined as $\tau_4 = 360 - (\alpha + \beta)/141$ where α and β are the two largest coordination angles in the four-coordinate species [50] lie in range 0.27–0.3. The planes of $N_{imine}–Cu–N_{imine}$ make an angle of 80.90°–81.53° with the planes of $N_{pyrrole}–Cu–N_{pyrrole}$. The metal–ligand interactions lead to a twisting of the ligand compared to the free ligand, which shows a mirror plane according its NMR spectrum. In this structure $Cu(2)L^2$ and $Cu(3)L^2$ units stack in an offset face-to-face fashion with displacement angle of 14.36°. Phenyl rings are nearly parallel to each other with an interplanar angle of 4.13° and the closest atom–atom distance is 3.79 Å. The mean centroid–centroid distance of 5.581 Å indicates very weak interactions between phenyl rings.

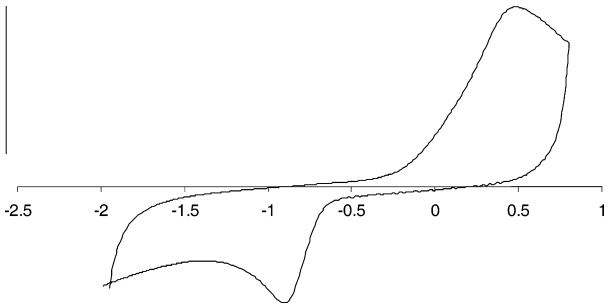

Fig. 3. Cyclic voltammogram of NiL^3 in DMF at a scan rate of 0.05 Vs^{-1}.

3.3. Geometry optimization and electronic and spectra structure

Selected geometric parameters of the fully optimized structure of CuL^2 are gathered in Table 4. There is good agreement between the observed and computed structural parameters. The imine and pyrrole nitrogens and the etheric oxygens of the complex have high negative atomic charges: −0.470, −0.50 and −0.54, respectively. The rather similar negative charge on the imine nitrogens and the formally anionic pyrrole nitrogens suggests that the latter donate more electron density to the copper atom, leading to rather strong $Cu–N_{pyrrole}$ bonding. This idea is supported by the short $Cu–N_{pyrrole}$ bond lengths in comparison to those of $Cu–N_{imine}$.

The TDDFT calculation shows that two long wavelength bands at 640.79 and 635.63 nm arise from transitions from the β-spin HOMO-19, HOMO-18 and HOMO, having mainly d_z^2, $d_{yz,xz}$ and π_{imine} characters, respectively, to the β-spin LUMO with dominant Cu d_{x^2-y2} character (see Supplementary material). The result is in

Table 5
Redox potentials (vs. Ag/Ag^+ electrode) in DMF.

Compound	Scan rate (m Vs^{-1})	Epa (V)	Epc(V)	$E_{1/2}$ (V)	ΔE (V)
NiL^1	50	not observed	−0.71045	–	–
	100	not observed	−0.80505	–	–
NiL^2	50	not observed	−0.788	–	–
	100	not observed	−0.808	–	–
NiL^3	50	0.402	−0.926	0.7	1.32
	100	0.627	−1.03	–	1.65
NiL^4	50	0.86	not observed	–	–
	100	not observed	not observed	–	–
Ferrocene	50	0.52	0.34	0.43	0.18

consistent with the observed broad band appeared in the visible region 620–670 nm, which can be assigned to the transitions from d_z^2, $d_{yz,xz}$ and π_{imine} to d_{x^2-y2}.

4. Cyclic voltammetry

The three ligands H_2L^2, H_2L^3 and H_2L^4 are irreversibly oxidized in DMF solvent. The respective anodic peak potentials at scan rate 0.05 Vs^{-1} are approximately 1.21, 1.24 and 1.22 V, respectively. The two ligands H_2L^1 and H_2L^2 also show irreversible reduction waves at approximately −1.27 and −1.8 V, respectively. Increasing scan rates give a positive peak potential shift for anodic peaks and a negative peak potential shift for cathodic peaks as well as increasing in current intensity.

The electrochemical properties of the nickel complexes were investigated in DMF with 0.1 M $LiClO_4$ as a supporting electrolyte: cyclic voltammetry data are summarized in Table 5. The two NiL^1 and NiL^2 complexes exhibit irreversible reduction waves but no anodic wave is observed. The NiL^4 complex, in contrast, exhibits only an irreversible anodic peak. The reduction of NiL^1 and NiL^2 (scan rate 0.05 Vs^{-1}) occurred at approximately −0.71 and −0.78 V, respectively, while the oxidation of NiL^4 occurs at 0.86 V. The NiL^3 complex shows a quasi-reversible anodic peak in 0.4 V and the corresponding cathodic peak in −0.92 V (Fig. 3). These results suggest that the complexes with softer thioethers are more easily oxidized than their oxygen analogs and stabilize higher oxidation states [51]. For low-oxidation states S ligands are expected to destabilize this state, as it is observed.

5. Conclusion

In the present work, we have synthesized and characterized new hexadentate ligands and their complexes with nickel(II) and copper(II) ions. Physico-chemical measurements confirm the 1:1 metal to ligand stoichiometry of the complexes. UV–Vis spectra and X-ray crystal structures indicate that the nickel complexes are in the distorted octahedral geometry while the copper complexes have a seesaw sawhorse coordination geometry. DFT calculations support that $N_{pyrrole}$–Cu bond lengths are shorter than the N_{imine}–Cu bonds and the calculated wavelengths for electronic transitions are in consistent with the observed broad absorption. Cyclic voltammetry results can suggest that softer thioethers are more easily oxidized than their oxygen analogs and stabilize higher oxidation states.

Acknowledgement

We are grateful to University of Tabriz Research Council for the financial support of this research.

Appendix A. Supplementary material

CCDC 611930 and 678398 contain the supplementary crystallographic data for NiL^3 and CuL^2. These data can be obtained free of charge from The Cambridge Crystallographic Data Centre via www.ccdc.cam.ac.uk/data_request/cif. Supplementary data associated with this article can be found, in the online version, at doi:10.1016/j.ica.2010.08.019.

References

[1] R. Drozdzak, B. Allaert, N. Ledoux, I. Dragutan, V. Dragutan, F. Verpoort, Coord. Chem. Rev. 249 (2005) 3055.
[2] E. Tsuchida, K. Oyaizu, Coord. Chem. Rev. 237 (2003) 213.
[3] S. Foster, A. Rieker, K. Maruyama, K. Murata, A. Nishinaga, J. Org. Chem. 61 (1996) 3320.
[4] J.S. Fossey, C.J. Richards, Tetrahedron Lett. 44 (2003) 8773.
[5] H. Kwong, L. Cheng, W. Lee, J. Mol. Catal. A: Chem. 150 (1999) 23.
[6] L. El-Sayed, H.A.M. Al-Gwidi, Energy Fuels 14 (2000) 179.
[7] P.S. Subramanian, E. Suresh, D. Srinivas, Inorg. Chem. 39 (2000) 2053.
[8] Z. Yang, R. Yang, F. Li, K. Yu, Polyhedron 19 (2000) 2599.
[9] M.R.A. Pillai, G. Samuel, S. Banerjee, B. Mathew, H.D. Sarma, S. Jurisson, Nucl. Med. Biol. 26 (1999) 69.
[10] M.R.A. Pillai, K. Kothari, B. Mathew, N.K. Pilkwal, S. Jurisson, Nucl. Med. Biol. 26 (1999) 233.
[11] M.R.A. Pillai, K. Kothari, Sh. Banerjee, G. Samuel, M. Suresh, H.D. Sarma, S. Jurisson, Nucl. Med. Biol. 26 (1999) 555.
[12] M.L. Golden, C.M. Whaley, M.V. Rampersad, J.H. Reibenspies, R.D. Hancock, M.Y. Darensbourg, Inorg. Chem. 44 (2005) 875.
[13] M. Cushmam, D. Yang, J.T. Mihalic, J. Chen, S. Gerhardt, R. Huber, M. Fischer, K. Kis, A. Bacher, J. Org. Chem. 67 (2002) 6871.
[14] P.A.N. Ready, M. Nethaji, A.R. Chakravarty, Inorg. Chem. 41 (2002) 450.
[15] P.L. Holland, W.B. Tolman, J. Am. Chem. Soc. 122 (2000) 6331.
[16] Y.J. Kim, S.O. Kim, Y.I. Kim, S.N. Choi, Inorg. Chem. 40 (2001) 4481.
[17] D.H. Nguyen, H. Hsu, M. Millar, S.A. Koch, J. Am. Chem. Soc. 118 (1996) 8963.
[18] C. Qiao, K. Ling, E.M. Shepard, D.M. Dooley, L.M. Sayrer, J. Am. Chem. Soc. 128 (2006) 6206.
[19] B.P. Hay, R.D. Hancock, Coord. Chem. Rev. 212 (2001) 61.
[20] A.T. Chaviara, E.E. Kioseoglou, A.A. Pantazaki, A.C. Tsipis, P.A. Karipidis, D.A. Kyriakidis, C.A. Bolos, J. Inorg. Biochem. 102 (2008) 1749.
[21] G. Brewer, C. Luckett, Inorg. Chim. Acta 358 (2005) 239.
[22] M.G. Bhowon, H. Li Kam Wah, A. Dosieah, M. Ridana, O. Ramalingum, D. Lacour, Synth. React. Inorg. Met.-Org. Chem. 34 (2004) 1.
[23] A. Sharma, A. Arora, K. Mathur, R.P. Mathur, Asian J. Chem. 15 (2003) 999.
[24] A. Sharma, A. Arora, K. Mathur, R.P. Mathur, Asian J. Chem. 15 (2003) 1091.
[25] Z.H. Chohan, H. Pervez, A. Rauf, A. Scozzafava, C.T. Supuran, J. Enzyme Inhib. Med. Chem. 17 (2002) 117.
[26] A. Datta, N. Kumar Karan, S. Mitra, V. Gramlich, J. Chem. Crystallogr. 33 (2003) 579.
[27] E. Kwiatkowski, M. Klein, G. Romanowski, Inorg. Chim. Acta 293 (1999) 115.
[28] C.A. Bolos, G.S. Nikolov, L. Ekateriniadou, A. Kortsaris, D.A. Kyriakidis, Met. Based Drug. 5 (1998) 323.
[29] C.I. Simionescu, M. Grigoras, I. Cianga, N. Olaru, Eur. Polymer J. 34 (1998) 891.
[30] M.A. Ali, K.R. Fernando, D. Palit, M. Nazimuddin, Transition Met. Chem. 20 (1995) 19.
[31] E. Kwiatkowski, M. Kwiatkowski, A. Olechnowicz, G. Bandoli, J. Chem. Crystallogr. 23 (1993) 473.
[32] A.S. Rothin, H.J. Banbery, F.J. Berry, T.A. Hamor, C.J. Jones, J.A. Mccleverty, Polyhedron 8 (1989) 491.
[33] N.A. Bailey, A. Barrass, D.E. Fenton, M.S. Leal Gonzalez, R. Moody, C.O. Rodriguez de Barbarin, J. Chem. Soc., Dalton Trans. (1984) 2741.
[34] A.A. Khandar, S.A. Hosseini-Yazdi, S.A. Zarei, Inorg. Chim. Acta 358 (2005) 3211.
[35] Bruker Saint-plas, Version 6.01, Data Reduction and Correction Program, Bruker AXS, Madison, WI, 1998.
[36] G.M. Sheldrick, Sadabs, Version 2.01, Bruker/Siemens Area Detector Absorpsion Correction Program, Bruker AXS, Madison, WI, 1998.
[37] G.M. Sheldrick, Shelxtl, version 5.10, Structure Determination software Suite, Bruker AXS, Madison, WI, 1998.
[38] International Tables for Crystallography, Tables 4.2.6.8 and 6.1.1.4, vol. C, Kluwer Academic Publishers, Dordrecht, Netherlands, 1992.
[39] P.A. Tasker, E.B. Fleischer, J. Am. Chem. Soc. 92 (1970) 7072.
[40] M. Kandaz, I. Yilmaz, S. Keskin, A. Koca, Polyhedron 21 (2002) 825.
[41] M.J. Frisch, G.W. Trucks, H.B. Schlegel, G.E. Scuseria, M.A. Robb, J.R. Cheeseman, J.A. Montgomery Jr., T. Vreven, K.N. Kudin, J.C. Burant, J.M. Millam, S.S. Iyengar, J. Tomasi, V. Barone, B. Mennucci, M. Cossi, G. Scalmani, N. Rega, G.A. Petersson, H. Nakatsuji, M. Hada, M. Ehara, K. Toyota, R. Fukuda, J. Hasegawa, M. Ishida, T. Nakajima, Y. Honda, O. Kitao, H. Nakai, M. Klene, X. Li, J.E. Knox, H.P. Hratchian, J.B. Cross, C. Adamo, J. Jaramillo, R. Gomperts, R.E. Stratmann, O. Yazyev, A.J. Austin, R. Cammi, C. Pomelli, J.W. Ochterski, P.Y. Ayala, K. Morokuma, G.A. Voth, P. Salvador, J.J. Dannenberg, V.G. Zakrzewski, S. Dapprich, A.D. Daniels, M.C. Strain, O. Farkas, D.K. Malick, A.D. Rabuck, K. Raghavachari, J.B. Foresman, J.V. Ortiz, Q. Cui, A.G. Baboul, S. Clifford, J. Cioslowski, B.B. Stefanov, G. Liu, A. Liashenko, P. Piskorz, I. Komaromi, R.L. Martin, D.J. Fox, T. Keith, M.A. Al-Laham, C.Y. Peng, A. Nanayakkara, M. Challacombe, P.M.W. Gill, B. Johnson, W. Chen, M.W. Wong, C. Gonzalez, J.A. Pople, Gaussian-03, Revision B.03, Gaussian Inc., Pittsburgh, PA, 2003.
[42] A.D. Becke, J. Chem. Phys. 98 (1993) 5648.
[43] C. Lee, W. Yang, R.G. Parr, Phys. Rev. B 37 (1988) 785.
[44] P. Comba, A. Lienke, Inorg. Chem. 40 (2001) 5206.
[45] M.E. Casida, Recent developments and applications in modern density functional theory, in: J.M. Seminario (Ed.), Theoretical and Computational Chemistry, vol. 4, Elsevier, Amsterdam, 1996.
[46] W.J. Geary, Coord. Chem. Rev. 7 (1971) 81.
[47] R.N. Patel, N. Singh, V.L.N. Gundla, Polyhedron 25 (2006) 3312.
[48] A.B.P. Lever, Inorganic Electronic Spectroscopy, second ed., Elsevier, Amsterdam, 1984.
[49] G. Rajsekhar, C.P. Rao, P. Saarenketo, K. Nattinen, K. Rissanen, New J. Chem. 28 (2004) 75.
[50] L. Yang, D.R. Powell, R.P. Houser, J. Chem. Soc., Dalton Trans. (2007) 955.
[51] G.J. Grant, M.W. Jones, K.D. Loveday, D.G. VanDerveer, W.T. Pennington, C.T. Eagle, L.F. Mehne, Inorg. Chim. Acta 300–302 (2000) 250.